

# UCLA

## UCLA Previously Published Works

### Title

Pathologic electrographic changes after experimental traumatic brain injury.

### Permalink

<https://escholarship.org/uc/item/73p5w4fq>

### Journal

Epilepsia, 57(5)

### ISSN

0013-9580

### Authors

Bragin, Anatol  
Li, Lin  
Almajano, Joyel  
et al.

### Publication Date

2016-05-01

### DOI

10.1111/epi.13359

Peer reviewed



## Pathologic electrographic changes after experimental traumatic brain injury

\*†Anatol Bragin, \*Lin Li, \*Joyel Almajano, \*Catalina Alvarado-Rojas, \*Aylin Y. Reid, \*Richard J. Staba, and \*†‡§Jerome Engel Jr.

*Epilepsia*, 57(5):735–745, 2016

doi: 10.1111/epi.13359

### SUMMARY

**Objective:** To investigate possible electroencephalography (EEG) correlates of epileptogenesis after traumatic brain injury (TBI) using the fluid percussion model.

**Methods:** Experiments were conducted on adult 2- to 4-month-old male Sprague-Dawley rats. Two groups of animals were studied: (1) the TBI group with depth and screw electrodes implanted immediately after the fluid percussion injury (FPI) procedure, and (2) a naive age-matched control group with the same electrode implantation montage. Pairs of tungsten microelectrodes (50  $\mu\text{m}$  outer diameter) and screw electrodes were implanted in neocortex inside the TBI core, areas adjacent to TBI, and remote areas. EEG activity, recorded on the day of FPI, and continuously for 2 weeks, was analyzed for possible electrographic biomarkers of epileptogenesis. Video-EEG monitoring was also performed continuously in the TBI group to capture electrographic and behavioral seizures until the caps came off (28–189 days), and for 1 week, at 2, 3, and 6 months of age, in the control group.

**Results:** Pathologic high-frequency oscillations (pHFOs) with a central frequency between 100 and 600 Hz, were recorded from microelectrodes, beginning during the first two post-FPI weeks, in 7 of 12 animals in the TBI group (58%) and never in the controls. pHFOs only occurred in cortical areas within or adjacent to the TBI core. These were associated with synchronous multiunit discharges and popSpikes, duration 15–40 msec. Repetitive pHFOs and EEG spikes (rHFOSs) formed paroxysmal activity, with a unique arcuate pattern, in the frequency band 10–16 Hz in the same areas as isolated pHFOs, and these events were also recorded by screw electrodes. Although loss of caps prevented long-term recordings from all rats, pHFOs and rHFOSs occurred during the first 2 weeks in all four animals that later developed seizures, and none of the rats without these events developed late seizures.

**Significance:** pHFOs, similar to those associated with epileptogenesis in the status rat model of epilepsy, may also reflect epileptogenesis after FPI. rHFOSs could be noninvasive biomarkers of epileptogenesis.

**KEY WORDS:** Traumatic brain injury, Epileptogenesis, Pathologic high frequency oscillations, Seizure, Electroencephalography, Spindles, Repetitive HFOs and spikes.



Anatol Bragin is a professional research neurologist in the Department of Neurology, David Geffen School of Medicine at UCLA.

Accepted February 19, 2016; Early View publication 25 March 2016.

\*Department of Neurology, University of California Los Angeles, Los Angeles, California, U.S.A.; †Brain Research Institute, University of California Los Angeles, Los Angeles, California, U.S.A.; ‡Departments of ‡Neurobiology and §Psychiatry and Biobehavioral Medicine, University of California Los Angeles, Los Angeles, California, U.S.A.

Address correspondence to Anatol Bragin and Jerome Engel Jr., Department of Neurology University of California Los Angeles, 710 Wetwood Plaza, Los Angeles CA 90095 U.S.A. E-mails: engel@ucla.edu; abragin@mednet.ucla.edu

Wiley Periodicals, Inc.

© 2016 International League Against Epilepsy

Traumatic brain injury (TBI) can be followed by multifaceted changes in the brain including axonal injury, cell death, and inflammation.<sup>1–3</sup> Among the multiple consequences of TBI are posttraumatic stress disorder, posttraumatic epilepsy (PTE), and high mortality rate.<sup>4–8</sup> Very little is known about the electrographic changes after TBI leading to PTE, and there are discrepancies in the descriptions of electrographic correlates of epilepsy after experimental TBI in rats. When TBI injury was performed in more caudal and

### KEY POINTS

- After FPI, pathologic high-frequency oscillations (pHFOs) occurred in, and adjacent to, TBI areas in all animals that developed late seizures
- Repetitive HFOs and EEG spikes (rHFOs), which reflect repeated population spikes associated with hypersynchronous multiunit discharges, were recorded from depth and screw electrodes in all animals that developed late seizures
- rHFOs could be a noninvasive biomarker of epileptogenesis

lateral parts of the brain,<sup>9–11</sup> clear epileptic seizure activity was observed. In experiments where TBI was performed in rostral parts of the brain, there is strong disagreement. Some authors report the occurrence of PTE.<sup>12–14</sup> However, other publications claim that electrographic events seen in this TBI model also occur in normal rats.<sup>15,16</sup>

The primary goal of the current experiments was to investigate changes in electroencephalography (EEG) during the first week after TBI induced by fluid percussion injury (FPI) and to identify those patterns that might be pathologic, and potential biomarkers of epileptogenesis. We specifically focused on paroxysmal delta activity, 10–20 Hz frequency band activity, which is in the sleep spindles frequency range and high-frequency oscillations (HFOs).

### METHODS

Experiments were conducted on 2- to 4-month-old male Sprague-Dawley rats. Three rats at age 8–10 months were added to the control group to investigate age-related spike-wave discharges (SWDs). All procedures were approved by the University of California Los Angeles Institutional Animal Care and Use Committee (protocol 2000-153). Rats were housed in transparent cages with food and water ad libitum in a standard environment with a 12 h/12 h light/dark cycle at 22°C. The light cycle started at 8 a.m. Thirty-two rats were randomly divided into two groups. The TBI group received FPI and were then immediately implanted with screw and depth electrodes in different areas of neocortex (Fig. S1A). The control group received the same electrode implantation montage without FPI, and also included three 8- to 10-month-old male Sprague-Dawley rats.

#### Induction of TBI

TBI was induced in rats using the lateral FPI method with a custom made pneumatic device. Rats ( $n = 18$ ) were anesthetized with 1.5–2.0 ml/min of isoflurane in 100% oxygen

and fixed in a stereotactic surgery frame. Body temperature was kept between 36.6 and 38.0°C with a thermostatically controlled heating pad. After exposure of the skull, a 3-mm-diameter craniotomy was centered 3 mm posterior to bregma and 6 mm lateral (left) to the midline. A plastic injury cap with a 3 mm opening was positioned over the craniotomy and affixed to the skull using silicone adhesive, cyanoacrylate glue, and dental cement. Once dried and securely affixed, the injury cap was filled with 0.9% saline and attached to the FPI pneumatic apparatus. Isoflurane was then discontinued and the level of responsiveness was monitored by the toe pinch reflex. At the first sign of responsiveness, FPI was delivered (pressure pulse duration 30 msec, 3.2–3.5 atm) to induce TBI. After impact the rat was monitored for duration of apnea and the time of first responsiveness to toe pinch. The rats were then placed back under isoflurane anesthesia and the injury cap was removed. Rats were investigated for the presence of any subdural blood and those rats with evidence of bleeding were excluded.

#### Implantation of electrodes

In the TBI group, following removal of the injury cap, the skull was cleaned and pairs of recording microelectrodes (tungsten 50  $\mu\text{m}$  outer diameter, with a 1 mm space between tips) were implanted in the center of the TBI core, as well as anterior (anteroposterior [AP] =  $-1.0$ , L = 6.0) and posterior (AP =  $-5.0$ ; L = 6.0) to the site of FPI, and in contralateral homotopic brain areas (AP =  $-3.0$ , L = 6.0). A pair of microelectrodes was also implanted in the left frontal cortex (LFC; AP =  $+3.0$ , L = 1.0), and recording screw electrodes were implanted lateral to the TBI core and in the right frontal cortex (Fig. S1A). The deeper recording site of the penetrating microelectrodes was located within layers 5–6 and the shorter was located in layers 1–2 of the neocortex. Ground and reference electrodes (stainless steel screws) were positioned in the cerebellum 2.0 mm posterior to lambda and 1.0 mm lateral from the sagittal suture. In the control group, electrodes were implanted using the same surgical procedures and coordinates as in the TBI group, but FPI was not performed.

After the last electrode was secured, the incision was sutured and treated with 0.25% bupivacaine as well as topical antibiotic ointment. Rats were placed in a heated cage and monitored for recovery before being returned to the home cage. Video-EEG recording of behavior and brain electrical activity began within an hour after completion of surgery and was performed continuously 24 h/day until the animal lost its cap, which varied from 28 to 189 days.

#### Data acquisition

EEG data were recorded with wide bandwidth from 0.1 Hz to 3.0 kHz and sampled at 10 kHz/channel (16 channels) using DataPac software, and stored on external hard drives. Parallel video recordings were carried out 24/7, which included infrared recordings to monitor behavior

during the dark phase. The main focus of the study was analysis of electrical activity during the first 2 weeks after FPI to reveal electrographic patterns that might predict epileptogenesis. The primary objective of subsequent continuous video-EEG monitoring was to document electrographic and behavioral seizure occurrence in the TBI rats; however, recordings were also analyzed for HFOs and oscillations in the frequency band 10–20 Hz (spindle frequency band) during this time. Rather than attempt to record from control animals for 6 months, groups of control animals were recorded continuously for 1 week at ages 2, 4, and 6 months to correspond roughly to the age range of injured rats in the continuously recorded TBI group (Table 1), and three rats, aged 8–10 months, were recorded for 1 h daily for 3 days to obtain representative SWDs for comparison purposes.

### Data analysis

Data analysis was performed blindly in such a way that one person (JA) was responsible for randomizing animals into TBI and control groups, and reviewing video-EEG data for existence or absence of seizures. Others (AB, CAR) performed analysis of electrical activity without knowledge of which animals were subjected to TBI and, of these, which animals had seizures.

For analysis of EEG activity, three 5–10 min duration files were selected manually on the day of surgery, and each of the following 2 weeks, obtained while animals were immobile and when they were awake exploring their home cage environment. The immobile period was characterized by the disappearance of theta activity and occurrence of high amplitude slow-wave activity, while during exploration theta activity was observed and most obvious on recording sites that were located above of hippocampus. The selection was verified by reviewing time frequency plots of selected files (Fig. S1B–D). The detection of the following electrographic events was performed in each animal: paroxysmal delta activity, sleep spindles, EEG spikes, and pHFOs (>100 Hz).

### Detection of seizures

For each rat, video-EEG data were reviewed manually each day to detect the occurrence electrographic and/or motor seizures using DataPac 2K2 software. Any high amplitude activity was reviewed in more detail, and the animal's behavior was verified in the video record. For EEG files containing seizures, the post-FPI day(s) of seizures were cataloged in an Excel Spreadsheet (Microsoft Corp.) and EEG files saved for further analysis. Seizures were

**Table 1. General description of experimental and control groups**

Rat ID	Age	TBI severity	Video-EEG days	Delta waves	pHFOs and rHFOs	Early SZ	Late SZ
<b>Control group</b>							
C1	2 month	NA	7	No	No	No	No
C2	2 month	NA	7	No	No	No	No
C3	2 month	NA	7	No	No	No	No
C4	2 month	NA	7	No	No	No	No
C5	2 month	NA	7	No	No	No	No
C6	2 month	NA	7	No	No	No	No
C7	3 month	NA	7	No	No	No	No
C8	3 month	NA	7	No	No	No	No
C9	3 month	NA	7	No	No	No	No
C10	6 month	NA	7	No	No	No	No
C11	6 month	NA	7	No	No	No	No
C12	6 month	NA	7	No	No	No	No
C13	6 month	NA	7	No	No	No	No
C14	6 month	NA	7	No	No	No	No
<b>TBI group</b>							
1	2 month	Mild	31	No	Yes	No	No
2	4 month	Severe	28	Yes	No	No	No
3	4 month	Severe	153	Yes	No	No	No
4	2 month	Severe	168 death	No	Yes	d4	d167
5	2.5 month	Severe	61	Yes	No	No	No
6	2 month	Severe	189	Yes	No	No	No
7	2.5 month	Severe	74 death	Yes	Yes	No	d74
8	2.5 month	Severe	63	Yes	Yes	d2	No
9	3 month	Severe	36 death	Yes	Yes	d0	d36
10	4 month	Mild	35 death	Yes	Yes	d1	d35
11	2 month	Moderate	64	Yes	No	No	No
12	2 month	Severe	63	Yes	Yes	d0&4	No

SZ, seizures; pHFOs, pathologic high-frequency oscillations; rHFOs, repetitive high frequency oscillations and spikes; TBI, traumatic brain injury.

defined as ictal EEG activity lasting >10 s, with or without behavioral correlates.

### Detection and analysis of sleep spindle activity

Each channel in the 5–10 min duration file was digitally band-passed filtered between 10 and 20 Hz (finite impulse response filter, roll-off, –33 dB/octave). Then the filtered signal was rectified and the root mean square amplitude (RMS; 700 msec sliding window) was calculated (DataPac software). Multiple filter cutoff frequencies and roll-off value combinations were tested to determine filter settings that would optimally pass the frequencies between 10 and 20 Hz. Successive RMS values >3 standard deviation (SD) above the mean value of the RMS signal (i.e., mean value calculated over the entire length of data file) and >600 msec in duration were detected and delimited by onset and offset boundary time markers as spindles. Consecutive events separated by <100 msec were combined as one event. Events not having a minimum of three waves >3 SD from the mean baseline signal and duration longer than 3 s were rejected from the analysis. This approach was effective in detecting >80% of spindle oscillatory events observable with visual EEG analysis. Each event was visually inspected to remove events that were contaminated by artifact, including movement, electronic, and other sources of signal noise.

### Detection of HFOs

Using a semiautomated computer software developed in our laboratory for HFO detection,<sup>17</sup> HFOs in the frequency band between 100 and 600 Hz were extracted from filtered signals and reviewed manually to remove false positives. HFOs with amplitude >2 SD above the mean baseline were considered as pHFOs. We measured the rate of occurrence, peak and mean frequency, and duration of detected pHFOs, and determined the proportion of recording sites in each animal which reliably recorded pHFOs.

### Analysis of multiunit recordings

For analysis of neuron discharges, the raw data were high-pass filtered (600 Hz) and multiunit activity was extracted by DataPac software. Data were considered to be multiunit activity if spikes with amplitudes twice as high as the microelectrode noise existed in the record.

### Analysis of detected events

For every channel in each archived EEG file, we performed power spectral analysis and correlation among spindle-frequency oscillations, HFOs, and multiunit activity using DataPac software and custom scripts in the Matlab program.

### Statistical analysis

For normally distributed data, we used paired and unpaired *t*-tests, or one-way analysis of variance (ANOVA) followed by post hoc Bonferroni tests. For data that failed

the normality test, Mann-Whitney or Wilcoxon tests were applied. A *p* < 0.05 level was accepted as indicating statistically significant differences.

### Histology

At the completion of monitoring, rats were deeply anesthetized with pentobarbital and transcardially perfused with phosphate-buffered saline and 4% paraformaldehyde. Brains were removed and post-fixed in 4% paraformaldehyde. They were then sectioned with 60  $\mu$ m slices using a Leica (Model, VT1000S) Vibratome, stained with cresyl-violet, and examined using a light microscope to determine the location of each electrode and to characterize cortical damage in relation to the injury site.

## RESULTS

### Number of animals

The TBI group consisted of 18 rats aged 2–4 months. Twelve survived FPI, and recordings from these rats were used in the analysis described in the following sections. The control group consisted of 14 rats aged 2–6 months on the day of surgery, and three rats aged 8–10 months at the time of recording.

### Sleep spindles in the control group

#### Appearance

Characteristics of sleep spindles from control animals, derived from seven consecutive days of video-EEG recording (Table 1), were consistent with published studies that described properties of sleep spindles in normal Sprague-Dawley rats recorded over a period of 2–6 months.<sup>18–20</sup> Sleep spindles were prominent when animals were immobile and had a mostly sinusoidal shape, with duration between 0.5 and 2.0 s and a rate of occurrence from 5.5 to 14.5/min (mean  $9.3 \pm 2.8$ /min). Power spectrograms were calculated from wide band recordings during periods of sleep spindles detected by software, and they consisted of oscillations in the frequency range 8–14 Hz with a clear dominant peak at 12–14 Hz, and in 21% of animals (*n* = 3) spectrograms contained two peaks at 7–8 Hz and 11–14 Hz (Fig. S2).

Some waves of the higher amplitude sleep spindles contained a sharp component, which met criteria for an EEG spike. To analyze parameters of spike components in sleep spindles in each control animal, single spindle waves with the 10% highest amplitude were selected, and the average duration of 1,703 sharp events was calculated to vary from 60 to 130 msec ( $88 \pm 17$ , mean  $\pm$  SD) (see examples in the Fig. S2). These sharp events in the control animals were not associated with pHFOs.

#### Spatial distribution

Spindles had the highest amplitude in the motor and frontal areas of neocortex. As published for human and rat sleep



spindles, we found these oscillations to be located under a single recording site or in several recording sites, ipsilaterally and bilaterally,<sup>21–23</sup> but they were not synchronized in all recording sites (see power spectrograms of all recording sites in all control rats in the Fig. S2).

### Sleep spindle oscillations in the TBI group

All TBI rats had sleep spindles with appearance and location similar to those in the control group. On the day of TBI, spindles were absent in four animals, and in the remaining animals their rate of occurrence was significantly lower than in the control group ( $5.6 \pm 2.6/\text{min}$  vs.  $9.3 \pm 2.9/\text{min}$ ;  $p = 0.0048$ ). During the following days, the rate of occurrence of sleep spindles increased in all animals and on days 5, 10, and 14, the mean rate was  $14.8 \pm 3.7$  events per min, which is significantly higher than in the control group ( $p = 0.0004$ ). Most sleep spindles had a duration from 0.5 to 1.5 s, but there was a significantly greater percentage of sleep spindles with a duration  $>1.5$  s in the TBI group compared to control group ( $p = 0.0089$ ). The central frequency of sleep spindles did not change dramatically after TBI. Power spectral analysis showed that within the first 2 weeks there was a peak in power between 12 and 14 Hz.

### Pathologic high-frequency oscillations

#### Appearance

pHFOs were observed in the neocortex of 7 of 12 animals in the TBI group (58%, Table 1), and in none of the control animals. Their frequency was between 80 and 300 Hz, which varied considerably, even within a single pHFO event (Fig. 1A). All pHFOs appeared during the first week (days 2–7). Animals that did not exhibit pHFOs during the first week never did during the subsequent recordings. They occurred when the animals were immobile and disappeared during exploration. When pHFOs appeared, they were associated initially with local negative EEG spikes (Fig. 1A). Some pHFOs were associated with local negative waves 300–600 msec in duration (Fig. 1B).

#### Spatial distribution

pHFOs occurred only in the TBI core of the neocortex and/or areas adjacent to the TBI. They were never found in LFC, or in the areas contralateral to the TBI. As recorded with pairs of tungsten electrodes located in the layers 2–3 and 5–6, pHFOs always had higher amplitude in the deeper layers of the neocortex. In the record presented in Figure 2A,B, pHFOs were recorded only in the area anterior to the TBI and did not propagate. These pHFOs oscillations may start abruptly with a high amplitude component (Fig. 2C top) or gradually increase in amplitude (Fig. 2C, the second line from the top) or have different intermediate forms. pHFOs were observed in the TBI area, as well as in sites adjacent to the TBI, and could propagate among these areas, but never to distant regions. An example is illustrated

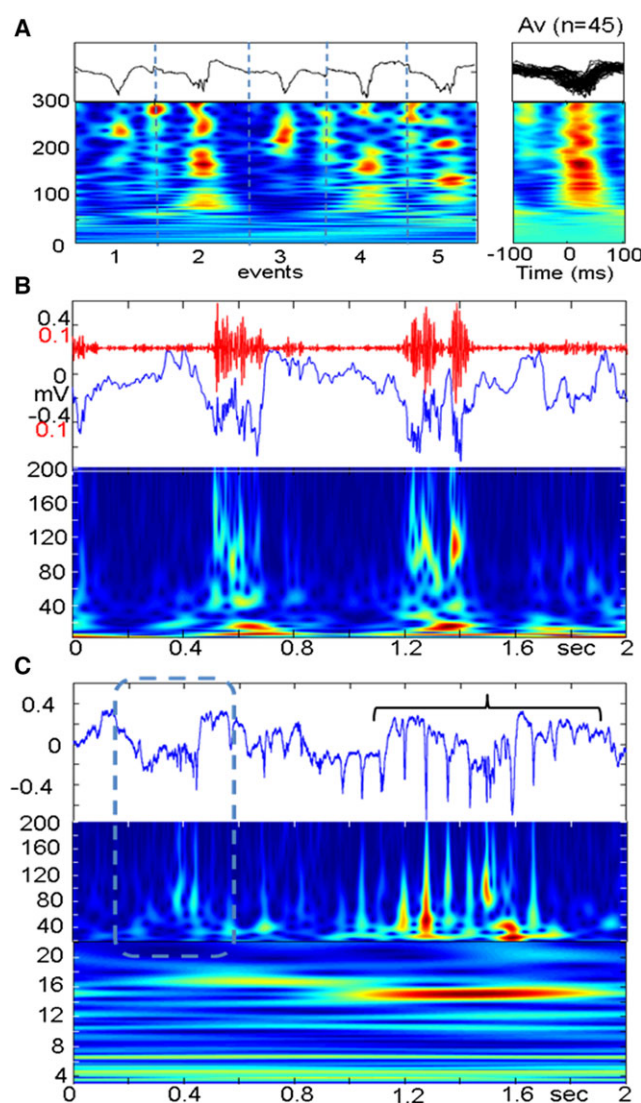


**Figure 1.**

(A) Pathologic high frequency oscillations (pHFOs) in the neocortex 3 days after FPI. (A) Five individual examples (black lines) and time frequency plots (below). (Right) time frequency plots of 45 pHFOs. (B) An example of pHFOs associated with a local slow-wave. (C) HFO (dashed box) followed by rHFOs (bracket) containing popSpikes.

*Epilepsia* © ILAE

in Figure 3 where pHFOs initially appeared in the deep electrode of the TBI core, and they spread to an adjacent recording site, but not to the LFC or contralateral areas. Although pHFOs were observed in electrodes located in both superficial (L1–2) and deep (L5–6) layers, they were associated only with increased synchronization of multiunit activity in L5–6.

### Repetitive HFOs and spikes (rHFOs)

A new pattern of paroxysmal activity occurred after TBI (Figs. 1C and 4A), within 1–3 days after the appearance of

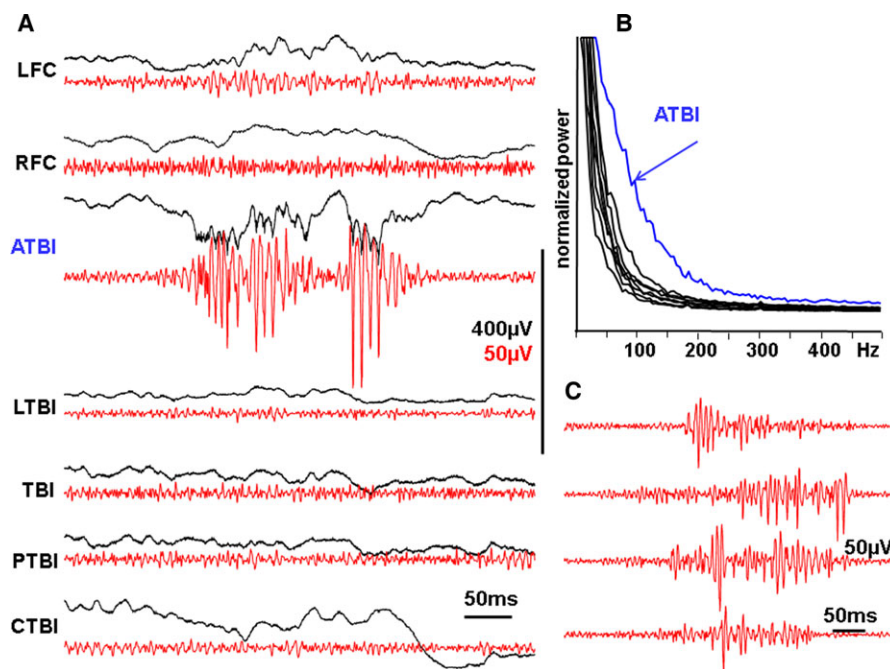


**Figure 2.**

(A) Local generation of pHFOs in the area adjacent to the traumatic brain injury on the 10th day after the injury. pHFOs appeared in the perilesional area anterior to the TBI core, but not in other areas of neocortex. Black lines are raw data recorded within a frequency band of 0.1 Hz–10 kHz, and red band pass (100–600 Hz). (B) Power spectrum density graph illustrating that the area generating pHFOs has higher power of electrical activity in the frequency band 60–300 Hz. (C) Examples of pHFOs, which have different patterns of evolution: descending, ascending, and mixed. LFC and RFC, left and right frontal cortex; ATBI, LTBI, and PTBI, areas adjacent to the TBI core from anterior and lateral and posterior sites sites; TBI, center of traumatic brain injury; CTBI, area homotopical to the TBI in the contralateral hemisphere.

*Epilepsia* © ILAE

pHFOs, which could be recorded from both micro and screw electrodes. This activity consisted of a series of rhythmic spikes of local field potentials within a frequency band of 10–16 Hz, with HFOs superimposed on each spike. This pattern was observed in every animal that exhibited pHFOs, and only in these animals. The sharp phase consisted of a spike, with a duration of 15–40 msec ( $25 \pm 11$ , mean  $\pm$  SD), which is similar to population spikes (popSpikes) described in our previous experiments in the kainate model of epilepsy<sup>24,25</sup> (Figs. 4B and S3A). The duration of the popSpikes component varied between 15 and 40 msec and was significantly shorter than the duration of sharp waves seen with high amplitude spindles in control animals ( $p = 0.00088$ ). The spike component of rHFOs was associated with pHFOs (Fig. 5A1) reflecting hypersynchronous discharges of local neurons. Figure 5A1,B illustrates that under high temporal resolution each spike of the rHFOs consisted of multiple sharp components, which represented summated action potentials from multiple neurons. The rate of rHFOs during immobility and slow-wave sleep did not differ significantly from the rate of sleep spindle in the TBI group. In addition to the presence of HFOs and synchrony of discharges of multiunit activity (Fig. S3B,C), there were several other differences between rHFOs and sleep spin-

dles that could be seen on skull screws. rHFOs could be recorded during the awake state, which never was observed for sleep spindles, as illustrated in Figure S4A,A1, where rHFOs occurred when theta rhythm was observed in adjacent neocortex. rHFOs had an arcuate shape, instead of the sinusoidal shape of sleep spindles (Figs. 4A and S3B), and rHFOs were localized to the TBI lesion, while sleep spindles were diffuse and bilateral.

rHFOs can also be distinguished from spike-wave discharges (SWDs), also known as high voltage spindles,<sup>26</sup> usually observed in older rats. As seen in three 8- to 10-month-old control rats, SWDs did not contain pHFOs (Fig. S4A,B). In addition, the frequency of SWDs was slower (6–9 Hz) than rHFOs (12–14 Hz), and SWDs never occurred during wakefulness.

### Recurrent paroxysmal delta activity

In 10 TBI animals (83%) recurrent paroxysmal 1–3 Hz delta activity was observed beginning immediately after FPI (Table 1, Fig. S5A,B). This activity remained for periods of several hours and decreased in amplitude or disappeared during walking, grooming, drinking, or eating. The maximum amplitude of this activity was in the TBI core and surrounding areas and it disappeared within 72–96 h after

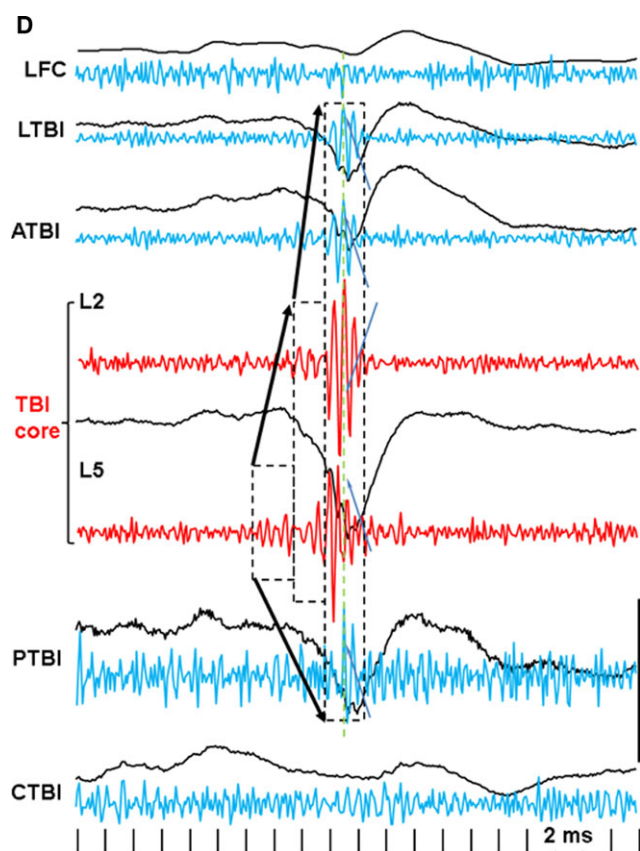


**Figure 3.**

An example of pHFO propagation in rat TBI-4. The pHFO is generated in the TBI area and propagates to adjacent areas but not distant areas. Dashed boxes outline the channels involved in the generation of pHFO. Black lines are raw data recorded within a frequency band 0.1 Hz–10 kHz, blue and red: band pass filtered at 100–600 Hz. Calibration scale is 0.5 mV for raw records, 0.1 mV for band pass filtered. Dashed boxes outline the number of recording sites where pHFOs were detected. Arrows indicate propagation of pHFOs. LFC, left frontal cortex; LTBI, neocortex lateral to the TBI core; ATBI, neocortex anterior to the TBI core; TBI, TBI core; PTBI, neocortex posterior to the TBI core; CTBI, neocortex in the homotopical point in the contralateral hemisphere.

*Epilepsia* © ILAE

FPI. The lower frequency EEG (<6 Hz) was relatively normal in the remote areas (i.e., ipsilateral frontal cortex and contralaterally).

## Seizures

### Early spontaneous seizures

Spontaneous seizures were observed within the first week after injury in five TBI animals (42%, see Table 1) and none of the controls. In these rats, EEG onset occurred simultaneously in all recorded sites and was characterized by the sudden occurrence of high amplitude spikes with a frequency 1–3 Hz. The duration of seizures ranged from 10 to 120 s (Fig. 6A). The only behavioral component of these seizures

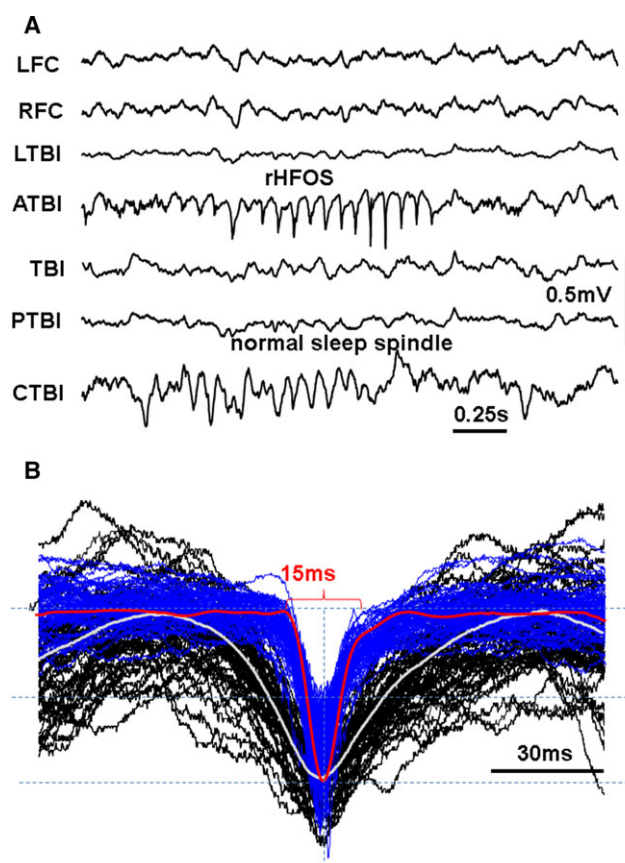


**Figure 4.**

(A) An example of rHFOS recorded 10 days after TBI in the area anterior to TBI (ATBI) and normal spindle that coincidentally occurred in the area contralateral to the TBI core (CTBI). (B) Fifty-five superimposed single waves from normal spindles (black) and rHFOSs. White and red thick lines are normalized averages of correspondingly normal and pathologic events.

*Epilepsia* © ILAE

was freezing, except for one animal that exhibited wet-dog shakes.

### Late spontaneous seizures

Four animals (30%) developed late spontaneous seizures. One of the four animals had two isolated seizures with a generalized EEG onset that was recorded on post-FPI day 91. This animal subsequently went into status epilepticus with a generalized ictal onset on day 167. Three other animals without prior evidence of late seizures went into status epilepticus on days 35, 36, and 74, respectively. An example of late seizure is presented in Figure 6B. In all four animals, a suppression of EEG amplitude occurred between 2 and 12 h before the status and onsets were generalized. Seizures occurred, in different animals, between one and 6 per hour for 8–10 h. All animals then remained in a comatose state with depressed EEG for 1–6 h, exhibited a few jerks, and died.



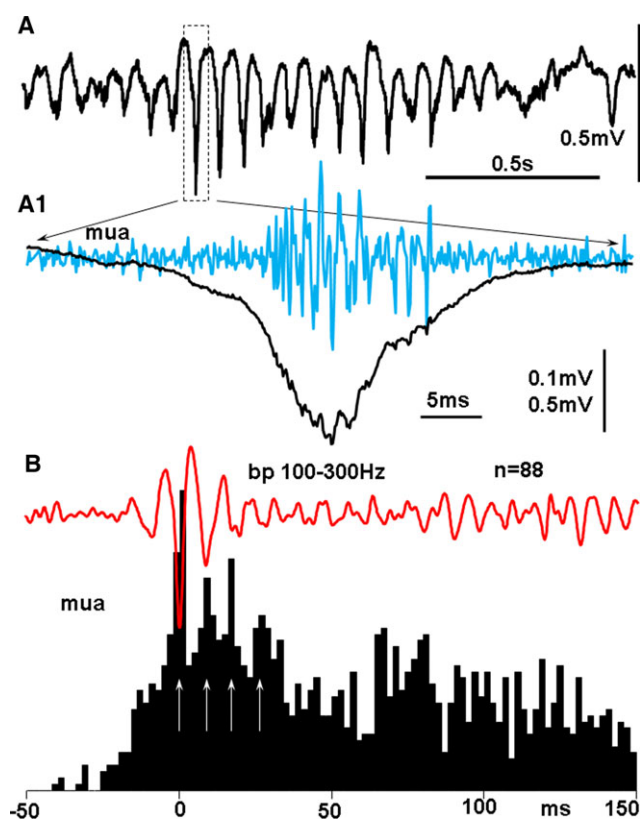


**Figure 5.**

(A) rHFOs recorded with a band pass 0.1 Hz–10 kHz. A1, black line: an expanded popSpike indicated by the dashed box. Blue line high passed (500 Hz) multiunit activity from the same electrode, indicating increased neuronal discharges during the spike of the rHFOs. (B) Red line: an average of 88 rHFOs; black: peri-event histogram of multiunit activity triggered by the peak of the largest spike of the rHFOs.

*Epilepsia* © ILAE

### Electrographic abnormalities as predictors of late seizure occurrence

Paroxysmal delta activity and early seizures appeared to have no predictive value for late seizures in this study (Table 1). On the other hand, all four rats that developed late seizures, on days 35, 36, 74, and 167, exhibited pHFOs and rHFOs during the first two post-FPI weeks (Table 1). Three rats with pHFOs and rHFOs did not have late seizures, but recording was discontinued on day 31 in one rat, and day 63 in two others, when their caps came off (Table 1). Given the recording schedules, it is not possible to know whether these rats, or those without early pHFOs and rHFOs, would have had late seizures if monitoring could have continued longer.

*Histologic evaluation* revealed varying degrees of local cell loss and encephalomalacia at the site of FPI. There was a correlation between severity of injury and the degree of tissue loss, cortical thinning, ventricular enlargement, and deformation of the hippocampus ipsilateral to the side of

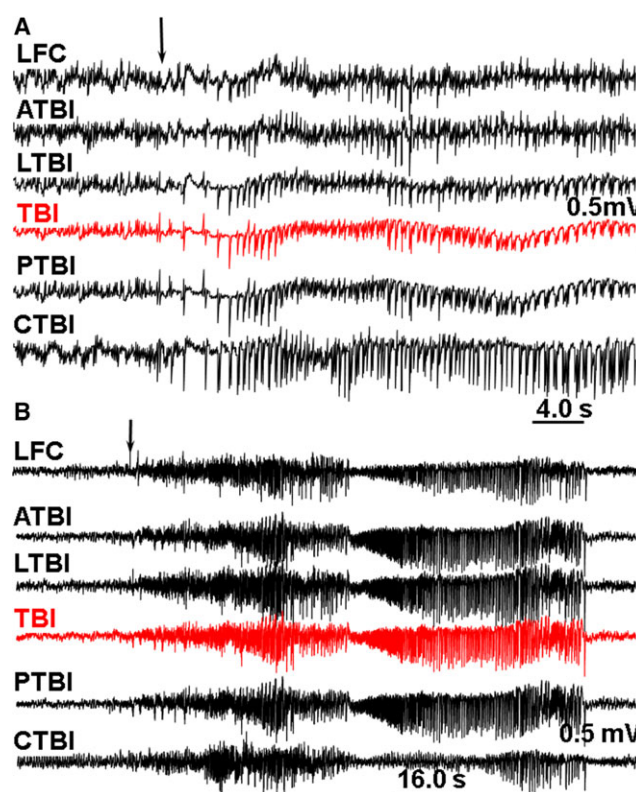


**Figure 6.**

(A) An example of spontaneous seizure on day 2 after TBI. (B) An example of seizure 167 days after FPI. LFC, and RFC: left and right frontal cortex; TBI, TBI core, place of application of FPI; ATBI, LTBI, PTBI and CTBI, correspond respectively to areas of neocortex anterior, lateral, posterior, and contralateral to the TBI core.

*Epilepsia* © ILAE

injury. No attempt was made to correlate the EEG findings reported here with lesion characteristics.

## DISCUSSION

The major finding of this study is that pathologic EEG changes occurred within the first 2 weeks after FPI in this rat model of TBI. pHFOs were recorded in 7 of 12 TBI rats, and never in controls. Within 1–3 days pHFOs clustered into repetitive spikes forming arcuate-shaped oscillations, termed rHFOs, where the sharp phase was a popSpike, reflecting pHFOs, and multiunit hypersynchrony in cortical layers 5–6. pHFOs and rHFOs were localized only to the TBI core and adjacent neocortex, and were present in all four rats that developed late seizures. Because rHFOs could be recorded from screw, as well as depth, electrodes, they may be noninvasive biomarkers of epileptogenesis.

pHFOs in this TBI rat model resemble pHFOs that occur in the rat status epilepticus models produced by kainic acid and pilocarpine, and are believed to be biomarkers of ictogenesis and epileptogenesis.<sup>27–30</sup> This suggests that the neuronal substrate of epileptogenesis after TBI is similar to that after KA lesion of hippocampus, and could indicate the for-

mation of pathologically interconnected clusters of neurons (PIN-clusters)<sup>29,31</sup> in the deep layers of neocortex, responsible for generating bursts of population spikes.

rHFOSs have not been described in the status models of hippocampal epilepsy and may be unique to neocortical epileptogenic mechanisms. Clear differences were documented between rHFOSs and normal sleep spindles, both of which occur in TBI animals. It is not clear if rHFOSs represent a new phenomenon or a transformation of normal spindles from a sinusoidal shape into the arcuate shape with a spike component, as a result of incorporation of repetitive popSpikes. The appearance of rHFOSs could suggest a disturbance in thalamocortical circuits after TBI, specifically in the nucleus reticularis, an important site involved in the generation and regulation of normal sleep spindles.<sup>26,32</sup>

The relationship between the rHFOSs reported here and the normal SWDs reported by some authors<sup>15,16</sup> to resemble what others have called ictal discharges following FPI<sup>12,13</sup> is not clear. High amplitude normal sleep spindles in our rats did, at times, contain sharp phases that could be considered “spikes.” These “spikes” were never associated with pHFOSs, and distinct differences in multiple parameters distinguished these normal oscillations from rHFOSs. SWDs typically occur in older rats (>6 months). Our experimental and control rats may have been too young to exhibit these events, or their absence could be explained by strain differences. We did, however, record SWDs from three older rats and determined that these oscillations also did not contain pHFOSs. The frequency of SWDs was slower than rHFOSs, and SWDs never occurred during wakefulness. SWDs could evolve from normal sleep spindles.

Late spontaneous seizures were observed in four TBI animals, and although all of these animals exhibited pHFOSs and rHFOSs, it is not possible to know whether more animals would have developed late seizures if their caps had not come off. Interpretation of the potential predictive value of these pathologic EEG events, therefore, is limited by difficulties inherent in continuous long-term video-EEG monitoring in rats. One of the four epileptic rats did not have the first late seizure until post-FPI day 91, whereas caps came off the three with early pHFOSs and rHFOSs and no late seizures on or before day 63. Although it is reasonable to argue that these rats might have developed late seizures if monitoring could have been continued, it is equally reasonable to argue that any, or all, of the five rats without pHFOSs and rHFOSs might have also developed late seizures. Further studies in which all the rats with and without early pHFOSs, and rHFOSs, are also recorded several months later, are needed, therefore, to definitively determine whether these pathologic EEG events are reliable biomarkers of epileptogenesis.

All four rats that had late seizures in this study developed status epilepticus and died. Englander et al. 2009 reported that mortality in patients with posttraumatic epilepsy after TBI was three times higher than in patients after TBI who

did not develop epilepsy.<sup>4,5</sup> The factors causing repeated seizures followed by death in our rats require further investigation.

The electrographic pattern of seizures described in our experiments is closer to what was described by Kharatishvili et al., and others<sup>9,10,33</sup> than by D’Ambrosio et al.<sup>12,13</sup> This might depend on the FPI coordinates. In our experiments they were caudolateral and could have involved more hippocampal damage as seen by Kharatishvili et al. and others,<sup>9–11,33</sup> whereas in experiments of D’Ambrosio they were more frontal and sagittal.<sup>12,13</sup> The degree to which the consequences of TBI depend on the location of the traumatic injury requires additional study.

Our observation of localized paroxysmal delta activity immediately following FPI in most rats is in agreement with data from posttraumatic patients.<sup>34–37</sup> This likely reflects nonspecific changes in the extracellular ionic and neurochemical milieu, leading to a transient suppression of synaptic activity and neuronal discharges<sup>3,35,38</sup>; with no effect on subsequent epileptogenic mechanisms.

As has been seen in patients, we observed early seizures within the first week in 29% of animals. Early seizures are reported to indicate an increased risk for late seizures in patients.<sup>38</sup> Perhaps a similar relationship might have been demonstrated if monitoring of these rats could have been continued longer.

In summary, we have demonstrated two pathologic EEG events occurring following FPI in our rat TBI model: pHFOSs resemble similar events in the status model of limbic epilepsy, and rHFOSs may be unique to neocortical epilepsy. rHFOSs are repetitive popSpikes associated with pHFOSs, and have been clearly distinguished from normal spindles. Further studies are needed to determine whether these events reliably predict the development of late seizures, but the fact that rHFOSs can be recorded from screw electrodes make them a candidate for a noninvasive biomarker of epileptogenesis.

## ACKNOWLEDGMENTS

This study was supported by the National Institutes of Health (NIH) National Institute of Neurological Disorders and Stroke (NINDS) grants NS065877 (AB); NS071048 and Citizens United for Research in Epilepsy (RS); NS033310 and NS080181 (JE). AYR was supported by a Clinical Fellowship award from Alberta Innovates-Health Solutions.

## DISCLOSURE

None of the authors has any conflicts of interests to disclosure. We confirm that we have read the Journal’s position on issues involved in ethical publication and affirm that this report is consistent with those guidelines.

## REFERENCES

1. Kharatishvili I, Pitkanen A. Posttraumatic epilepsy. *Curr Opin Neurol* 2010;23:183–188.

2. Loscher W, Brandt C. Prevention or modification of epileptogenesis after brain insults: experimental approaches and translational research. *Pharmacol Rev* 2010;62:668–700.
3. Giza CC. Post-traumatic epileptogenesis: good and bad plasticity. In Rho JMSR, Stafstrom CE (Ed) *Epilepsy: mechanisms, models and translational perspectives*. Boca Raton, FL: CRC Press, Taylor and Francis Group LLC, 2010:181–208.
4. Harrison-Felix C, Whiteneck G, Devivo MJ, et al. Causes of death following 1 year postinjury among individuals with traumatic brain injury. *J Head Trauma Rehabil* 2006;21:22–33.
5. Englander J, Bushnik T, Wright JM, et al. (2009) Mortality in late post-traumatic seizures. *J Neurotrauma* 26:1471–1477.
6. Agrawal A, Timothy J, Pandit L, et al. Post-traumatic epilepsy: an overview. *Clin Neurol Neurosurg* 2006;108:433–439.
7. Thapa A, Chandra SP, Sinha S, et al. (2010) Post-traumatic seizures: a prospective study from a tertiary level trauma center in a developing country. *Seizure* 19:211–216.
8. Annegers JF, Hauser WA, Coan SP, et al. A population-based study of seizures after traumatic brain injuries. *N Engl J Med* 1998;338:20–24.
9. Kharatishvili I, Nissinen JP, McIntosh TK, et al. A model of posttraumatic epilepsy induced by lateral fluid-percussion brain injury in rats. *Neuroscience* 2006;140:685–697.
10. Shultz SR, Cardamone L, Liu YR, et al. Can structural or functional changes following traumatic brain injury in the rat predict epileptic outcome? *Epilepsia* 2013;54:1240–1250.
11. Statler KD, Scheerlinck P, Pouliot W, et al. A potential model of pediatric posttraumatic epilepsy. *Epilepsy Res* 2009;86:221–223.
12. D'Ambrosio R, Fairbanks JP, Fender JS, et al. Post-traumatic epilepsy following fluid percussion injury in the rat. *Brain* 2004;127:304–314.
13. D'Ambrosio R, Fender JS, Fairbanks JP, et al. Progression from frontal-parietal to mesial-temporal epilepsy after fluid percussion injury in the rat. *Brain* 2005;128:174–188.
14. D'Ambrosio R, Hakimian S, Stewart T, et al. Functional definition of seizure provides new insight into post-traumatic epileptogenesis. *Brain* 2009;132:2805–2821.
15. Pearce PS, Friedman D, LaFrancois JJ, et al. Spike-wave discharges in adult Sprague-Dawley rats and their implications for animal models of temporal lobe epilepsy. *Epilepsy Behav* 2014;32:121–131.
16. Rodgers KM, Dudek FE, Barth DS. Progressive, seizure-like, spike-wave discharges are common in both injured and uninjured sprague-dawley rats: implications for the fluid percussion injury model of post-traumatic epilepsy. *J Neurosci* 2015;35:9194–9204.
17. Staba RJ, Wilson CL, Bragin A, et al. Quantitative analysis of high-frequency oscillations (80–500 Hz) recorded in human epileptic hippocampus and entorhinal cortex. *J Neurophysiol* 2002;88:1743–1752.
18. Pinault D, Slezia A, Acsady L. Corticothalamic 5–9 Hz oscillations are more pro-epileptogenic than sleep spindles in rats. *J Physiol* 2006;574:209–227.
19. van Luijckelaar EL. Spike-wave discharges and sleep spindles in rats. *Acta Neurobiol Exp (Wars)* 1997;57:113–121.
20. Willoughby JO, Mackenzie L. Nonconvulsive electrocorticographic paroxysms (absence epilepsy) in rat strains. *Lab Anim Sci* 1992;42:551–554.
21. Andrillon T, Nir Y, Staba RJ, et al. Sleep spindles in humans: insights from intracranial EEG and unit recordings. *J Neurosci* 2011;31:17821–17834.
22. Sitnikova E, Hramov AE, Grubov V, et al. Time-frequency characteristics and dynamics of sleep spindles in WAG/Rij rats with absence epilepsy. *Brain Res* 2014;1543:290–299.
23. Mölle M, Eschenko O, Gais S, et al. The influence of learning on sleep slow oscillations and associated spindles and ripples in humans and rats. *Eur J Neurosci* 2009;29:1071–1081.
24. Bragin A, Benassi SK, Kheiri F, et al. Further evidence that pathologic high-frequency oscillations are bursts of population spikes derived from recordings of identified cells in dentate gyrus. *Epilepsia* 2011;52:45–52.
25. Bragin A, Wilson CL, Engel J. Voltage depth profiles of high-frequency oscillations after kainic acid-induced status epilepticus. *Epilepsia* 2007;48:35–40.
26. Kandel A, Buzsaki G. Cellular-synaptic generation of sleep spindles, spike-and-wave discharges, and evoked thalamocortical responses in the neocortex of the rat. *J Neurosci* 1997;17:6783–6797.
27. Bragin A, Engel J Jr, Wilson CL, et al. Hippocampal and entorhinal cortex high-frequency oscillations (100–500 Hz) in human epileptic brain and in kainic acid-treated rats with chronic seizures. *Epilepsia* 1999;40:127–137.
28. Bragin A, Wilson CL, Almajano J, et al. High-frequency oscillations after status epilepticus: epileptogenesis and seizure genesis. *Epilepsia* 2004;45:1017–1023.
29. Bragin A, Wilson CL, Engel J Jr. Chronic epileptogenesis requires development of a network of pathologically interconnected neuron clusters: a hypothesis. *Epilepsia* 2000;41:S144–S152.
30. Mazarati A, Bragin A, Baldwin R, et al. Epileptogenesis after self-sustaining status epilepticus. *Epilepsia* 2002;43(Suppl. 5):74–80.
31. Bragin A, Mody I, Wilson CL, et al. Local generation of fast ripples in epileptic brain. *J Neurosci* 2002;22:2012–2021.
32. Barthó P, Slézia A, Máttyás F, et al. Ongoing network state controls the length of sleep spindles via inhibitory activity. *Neuron* 2014;82:1367–1379.
33. Kharatishvili I, Pitkanen A. Association of the severity of cortical damage with the occurrence of spontaneous seizures and hyperexcitability in an animal model of posttraumatic epilepsy. *Epilepsy Res* 2010;90:47–59.
34. Moeller F, Moehring J, Ick I, et al. EEG-fMRI in atypical benign partial epilepsy. *Epilepsia* 2013;54:103–108.
35. Ronne-Engstrom E, Winkler T. Continuous EEG monitoring in patients with traumatic brain injury reveals a high incidence of epileptiform activity. *Acta Neurol Scand* 2006;114:47–53.
36. Vespa PM, Miller C, McArthur D, et al. Nonconvulsive electrographic seizures after traumatic brain injury result in a delayed, prolonged increase in intracranial pressure and metabolic crisis. *Crit Care Med* 2007;35:2830–2836.
37. Vespa PM, Nuwer MR, Nenov V, et al. Increased incidence and impact of nonconvulsive and convulsive seizures after traumatic brain injury as detected by continuous electroencephalographic monitoring. *J Neurosurg* 1999;91:750–760.
38. Beghi E. Overview of studies to prevent posttraumatic epilepsy. *Epilepsia* 2003;44(Suppl. 10):21–22.

## SUPPORTING INFORMATION

Additional Supporting Information may be found in the online version of this article:

**Figure S1.** (A) Schematic illustration of the location of the fluid percussion injury (red circle) and the location of the implanted electrodes. Two attached circles symbolize pairs of 50  $\mu\text{m}$  tungsten microelectrodes with 1.0 mm separation between the tips. Circles with a cross symbolize screw electrodes. TBI, traumatic brain injury; A, anterior; C, contralateral; L, lateral; P, posterior. LFC and RFC are correspondingly left and right frontal cortex. (B) Representative of normalized power histograms during immobility acquired every 1 h during a 24 h time period. (C) An example of raw electrical activity during awake and immobility. (D) Time frequency plot of activity presented in part C. Stars indicate some spindle oscillations selected for data analysis.

**Figure S2.** Power spectrograms and duration of spikes of sleep spindles of normal rats of three different ages: 2, 4, and 6 months (indicated at the top).

**Figure S3.** Electrographic correlates of areas generating pHFOs.

**Figure S4.** (A) An example of rHFOS (ATBI, red line) occurrence during awake (theta) state. Most clear theta

activity was observed in the area posterior to the TBI core (PTBI). A1: time-frequency plot of rPHOS with the base frequency 12 Hz (green dashed line). Inset illustrates power spectra density plot of 1 min of awake state with peak at 13 Hz in ATBI and peak 7 Hz in PTBI. **(B)** An example of SWD pattern recorded in an 8-month-old rat. B1: time-frequency plot of LMC activity with the base line at 7 Hz (green dashed line). Inset: power spectra density plot of all six channels illustrating a peak at 7 Hz. The peak at 14 Hz is a second harmonic of the first peak.

**Figure S5.** **(A)** Recurrent paroxysmal delta activity (RPDA) 24 h after FPI. This activity has a maximum amplitude in the TBI core and adjacent areas. It is negligible or absent in the remote (LFC) ipsilateral or in the contralateral hemisphere (RFC and CTBI), and normal sleep spindle activity in these areas may appear during RPDA (arrow on the top). **(B)** Normalized power spectrograms in different recording sites for a 5 min period of RPDA.